LETTER

doi:10.1038/nature12526

Type 2 innate lymphoid cells control eosinophil homeostasis

Jesse C. Nussbaum[1], Steven J. Van Dyken[1], Jakob von Moltke[1], Laurence E. Cheng[2], Alexander Mohapatra[3], Ari B. Molofsky[4], Emily E. Thornton[5], Matthew F. Krummel[5], Ajay Chawla[1,6,7], Hong-Erh Liang[1] & Richard M. Locksley[1,3,8]

Eosinophils are specialized myeloid cells associated with allergy and helminth infections. Blood eosinophils demonstrate circadian cycling, as described over 80 years ago[1], and are abundant in the healthy gastrointestinal tract. Although a cytokine, interleukin (IL)-5, and chemokines such as eotaxins mediate eosinophil development and survival[2], and tissue recruitment[3], respectively, the processes underlying the basal regulation of these signals remain unknown. Here we show that serum IL-5 levels are maintained by long-lived type 2 innate lymphoid cells (ILC2) resident in peripheral tissues. ILC2 cells secrete IL-5 constitutively and are induced to co-express IL-13 during type 2 inflammation, resulting in localized eotaxin production and eosinophil accumulation. In the small intestine where eosinophils and eotaxin are constitutive[4], ILC2 cells co-express IL-5 and IL-13; this co-expression is enhanced after caloric intake. The circadian synchronizer vasoactive intestinal peptide also stimulates ILC2 cells through the VPAC2 receptor to release IL-5, linking eosinophil levels with metabolic cycling. Tissue ILC2 cells regulate basal eosinophilopoiesis and tissue eosinophil accumulation through constitutive and stimulated cytokine expression, and this dissociated regulation can be tuned by nutrient intake and central circadian rhythms.

Eosinophils require survival signals delivered through the common β-receptor chain (βc) shared by IL-3, IL-5 and granulocyte–macrophage colony-stimulating factor (GM-CSF)[1]. IL-5 is particularly important, as supported by studies in IL-5-deficient[5] and IL-5 receptor α chain (IL-5Rα)-deficient[6] mice, and in humans using anti-IL-5 and anti-IL-5Rα antibodies that target eosinophils in disease. Without IL-5 signalling, residual eosinophils have been attributed to IL-3 and GM-CSF, as well as eosinophil chemokines, such as eotaxins, that sequester these cells into tissues[1,3].

To identify cells that support eosinophils, we generated IL-5 reporter mice, designated Red5 (recombinase-expressing detector for IL-5; R5)[7]. Cells from these mice contain a tandem dimer red fluorescent protein (tdTomato) linked by an internal ribosomal entry site (IRES) to a Cre element replacing the translation initiation site of the endogenous *Il5* gene, facilitating function marking, fate mapping and deletion based on IL-5 expression (Fig. 1a). We validated that the construct disrupts the endogenous *Il5* gene and that R5 fluorescence correlates with IL-5 production using $CD4^+$ T cells examined after T-helper type 1 (T_H1) or T-helper type 2 (T_H2) polarization (Extended Data Fig. 1a–c).

Consistent with previous observations[8], $CD45^+R5^+CD4^-$ cells were present in non-lymphoid tissues, including the brain, heart, lung, kidney, skin, intestine and uterus, whereas few $R5^+$ cells were in lymphoid organs, including spleen, bone marrow, lymph nodes or thymus, or in the liver (Fig. 1b, c). In all tissues, the vast majority of $R5^+$ cells were small cells (forward-/side-scatter low) that lacked lineage markers for T, B, natural killer (NK) and myeloid cells, and expressed markers for innate lymphoid type 2 cells (ILC2)[9], including CD90.2 (Thy1), CD127 (IL-7Rα), KLRG1 and ICOS; T1/ST2 and CD25 expression varied among tissues

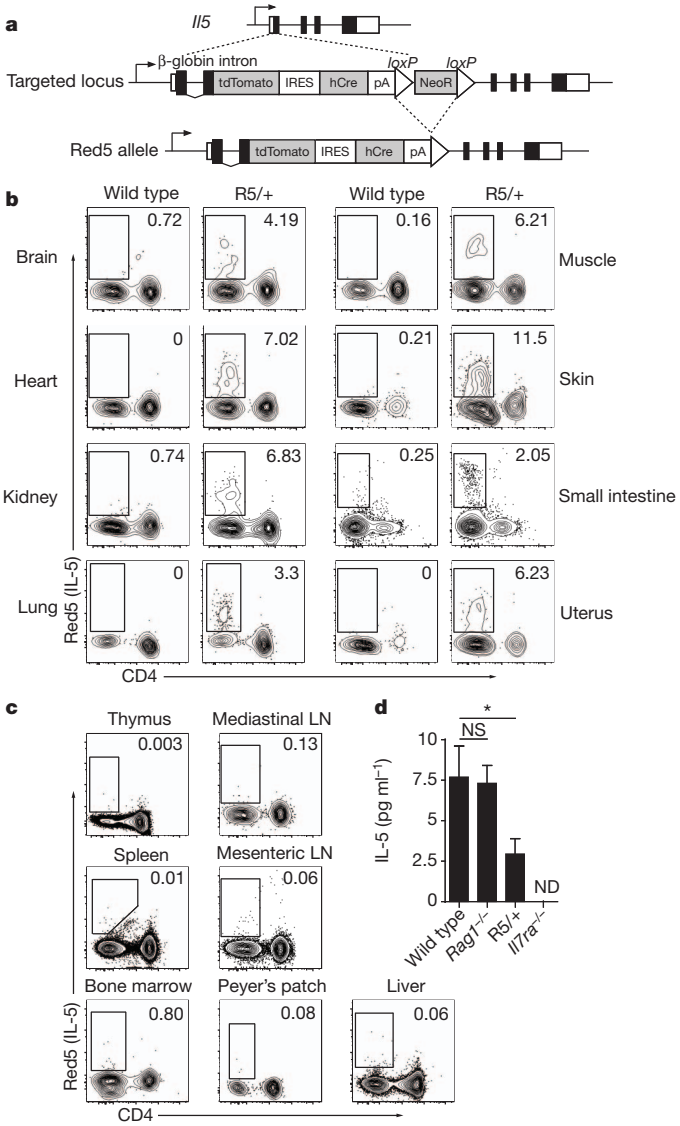

Figure 1 | Innate cells produce IL-5 in tissues at rest. **a**, Schematic of targeting construct. **b**, **c**, Flow cytometry of tissues, previously gated on $CD45^+CD90.2^+$ cells in wild-type and R5/+ (**b**) or $CD90.2^+$ cells in R5/R5 (**c**) naive mice. **d**, Serum IL-5. Data are representative of two independent experiments with two mice per group (**b**–**d**) or pooled from three independent experiments for 7 (wild type), 4 (Red5), or 8 (others) mice per group (**c**). Represented as mean ± s.e.m. LN, lymph nodes; ND, none detected; NS, not significant; $*P < 0.05$ by Student's *t*-test.

[1]Department of Medicine, University of California San Francisco, San Francisco, California 94143-0795, USA. [2]Department of Pediatrics, University of California San Francisco, San Francisco, California 94143-0795, USA. [3]Departments of Microbiology & Immunology, University of California San Francisco, San Francisco, California 94143-0795, USA. [4]Department of Laboratory Medicine, University of California San Francisco, San Francisco, California 94143-0795, USA. [5]Department of Pathology, University of California San Francisco, San Francisco, California 94143-0795, USA. [6]Department of Physiology, University of California San Francisco, San Francisco, California 94143-0795, USA. [7]Cardiovascular Research Institute, University of California San Francisco, San Francisco, California 94143-0795, USA. [8]Howard Hughes Medical Institute, University of California San Francisco, San Francisco, California 94143-0795, USA.

but was present on all lung R5$^+$ ILC2 cells (Extended Data Fig. 2a). Most (75–80%) CD90.2$^+$T1/ST2$^+$ lung ILC2 cells were R5$^+$, and these cells had the highest reporter expression compared to the few ILC2 cells from bone marrow and lymph nodes (Extended Data Fig. 2b). Sorted R5/+ ILC2 cells spontaneously secreted IL-5 in culture, confirming that the reporter marks IL-5 production (Extended Data Fig. 2c). Consistent with previous reports[9], numbers of ILC2 and R5$^+$ ILC2 cells were similar in recombinase activating gene (RAG)-deficient mice but were nearly absent in CD127-deficient mice (Extended Data Fig. 3a–c). Correspondingly, serum IL-5 was comparable in wild-type and RAG-deficient mice, reduced to about half-normal levels in heterozygous R5/+ mice, and was not detected in CD127-deficient mice (Fig. 1d).

Few ILC2 cells were present in the lungs of newborn mice, but within the first week CD90.2$^+$T1/ST2$^+$ cells increased, and the percentage that were R5$^+$ reached adult levels (Fig. 2a and Extended Data Fig. 3d–e). We administered 5-bromodeoxyuridine (BrdU) in drinking water of adult mice for 2 weeks to label dividing cells and found that less than 10% of lung ILC2 cells were labelled (Extended Data Fig. 3f). Pulse–chase labelling indicated that the decay of labelled ILC2 cells was substantially slower than CD4$^+$ T cells (Fig. 2b). As assessed using multiphoton microscopy, lung R5$^+$ ILC2 cells were embedded in collagen-rich regions near the confluence of medium-sized blood vessels and airways but were absent from alveoli (Fig. 2c and data not shown).

Lung eosinophilia is a hallmark of allergic lung disease and helminth migration, but eosinophils are rare in the lung at baseline[1] despite constitutive local IL-5. In previous studies, ILC2 cells stimulated with cytokines or helminth infection upregulated IL-13 (refs 10, 11), which is genetically linked to IL-5 in mice and humans and induces epithelial eotaxins (including CCL11) and endothelial adhesins necessary for eosinophil trafficking[1,3]. We crossed R5 mice to Smart13 (also called *Il13*$^{tm2.1Lky}$) reporter mice, in which non-signalling human CD4 marks cells producing IL-13 (ref. 11). In contrast to resting ILC2 cells, lung ILC2 cells expressed the IL-13 reporter after infection with the helminth *Nippostrongylus brasiliensis*. All IL-13$^+$ ILC2 cells in the lung were R5$^+$, whereas CD4$^+$ T cells expressed IL-5, IL-13, or both cytokines, consistent with previous observations (Fig. 3a)[11].

We crossed R5/R5 mice to mice carrying a ROSA26-flox stop-YFP allele to fate-map cells that expressed the IL-5-linked Cre recombinase, and infected the mice with *N. brasiliensis* to elicit a type 2 immune response. After infection, YFP was present only in ILC2 cells and CD4$^+$ T cells, and all YFP$^+$ cells were also R5$^+$ (Extended Data Fig. 4a, b). We also crossed R5/R5 mice to mice carrying a ROSA26-flox stop-diphtheria toxin A allele to delete IL-5-producing cells. The R5 allele was designed such that expression of the tdTomato reporter precedes Cre-mediated *loxP* recombination. Therefore, in R5/R5 deleter mice, a population of R5^{lo} cells may be detectable before they express the ROSA26-diphtheria toxin. At baseline, R5/R5 and R5/R5 deleter mice had comparable numbers of total cells and CD4$^+$ T cells in the bone marrow, spleen, lung and small intestine lamina propria (Extended Data Fig. 4c), but R5$^+$ ILC2 cells were deleted in the lung (Fig. 3b) and small intestine (Extended Data Fig. 4d).

To study the activity of lung ILC2 cells in the absence of T_H2 cells, we crossed R5/R5 and R5/R5 deleter mice onto a RAG-deficient background and administered IL-2 and IL-33 (refs 10, 12, 13). As expected, cytokine-activated ILC2 cells in R5/R5 RAG-deficient mice showed increased surface KLRG1 expression and R5 mean fluorescence intensity (Extended Data Fig. 5). Cytokine administration increased the ILC2 population and induced eotaxin-1 (CCL11) in lungs of R5/R5 RAG-deficient mice but not in RAG-deficient R5/R5 deleter mice (Fig. 3c). ILC2 cell deficiency was bypassed by administering IL-13, which partially restored eotaxin levels.

Whereas eosinophils are rare in the lung at baseline, they are abundant in other tissues, such as the small intestine lamina propria, where they depend on CCL11 (ref. 4), and are absent in mice that lack ILC2 cells (refs 13, 14). Our finding that ILC2 cells in the lung can control

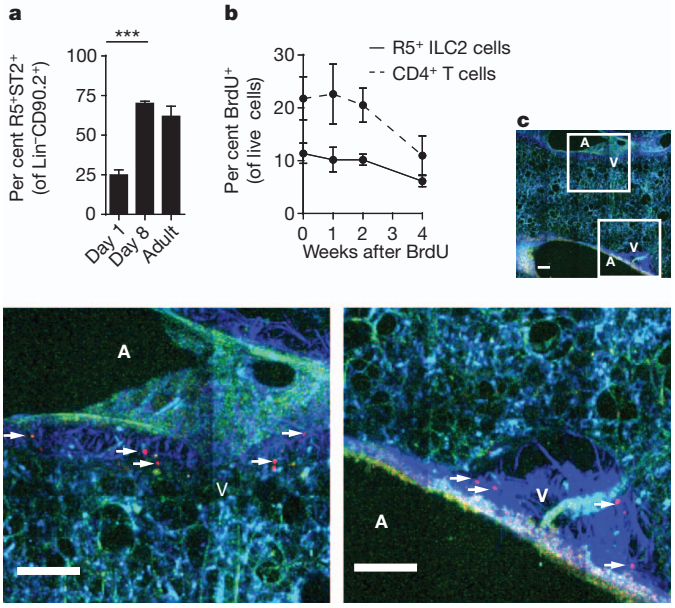

Figure 2 | ILC2 cells expand after birth and persist in collagen-rich structures. a, Per cent of lung Lin$^-$CD90.2$^+$ cells R5$^+$T1/ST2$^+$ on day 1, day 8, or week 8. **b**, Per cent BrdU$^+$ of R5$^+$ ILC2 cells and total CD4$^+$ cells in lung after 4 weeks BrdU. **c**, Representative multiphoton images of tdTomato fluorescence (red) in naive R5/R5 actin–CFP mice; CFP and autofluorescence in blue and green, respectively. A, airway; V, vasculature. Collagen second harmonic appears blue. Scale bars, 100 μm. Data are pooled from three independent experiments for 5 (day 1), 6 (day 8), or 4 (adult) mice per group (**a**); or pooled from two independent experiments for 5 (week 0), 6 (week 1), or 3 (others) mice per group (**b**). Represented as mean ± s.e.m. Images represent eight regions taken from two mice. Lin, lineage markers (B220, CD5, CD11b, CD11c, Ly6G, FcεRI and NK1.1); ***$P < 0.01$ by Student's *t*-test.

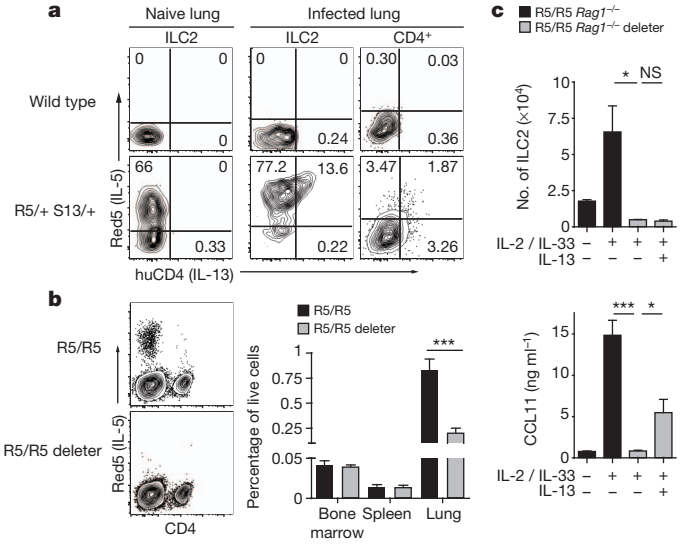

Figure 3 | IL-5 and IL-13 co-expression in lung ILC2. a, Lung IL-5 and IL-13 reporter expression before and after infection. **b**, Flow cytometry of CD90.2$^+$ lung cells and per cent with ILC2 surface markers (CD90.2 and either KRLG1, T1/ST2 or CD25) at rest. **c**, ILC2 (left lung) and CCL11 concentration (right lung) after IL-2, IL-33 and IL-13 treatment. Data are representative of three independent experiments with 4 (naive R5$^+$Smart13$^+$ (S13$^+$)), 5 (infected R5$^+$Smart13$^+$), or 2 (others) mice per group (**a**), pooled from three independent experiments for 6 (R5/R5 bone marrow and spleen) or 9 (all others) mice per group (**b**), or pooled from two independent experiments for 8 (R5/R5 + IL-2/IL-33), 5 (R5/R5 deleter + IL-2/IL-33/IL-13), or 3 (others) mice per group (**c**). Represented as mean ± s.e.m. huCD4, human CD4; NS, not significant; *$P < 0.05$; ***$P < 0.001$, by Student's *t*-test.

eosinophil recruitment through dissociated expression of IL-5 and IL-13 led us to explore the role of ILC2-derived cytokines in the basal regulation of peripheral eosinophils. We measured serum IL-5 levels at 10:00 and at 22:00 and found that the levels correlated with the circadian variation in blood eosinophils[15]. Although influenced by the adrenal–cortical axis[15], blood eosinophils can be dominantly synchronized by meal timing[16]. Mice fasted for 16 h showed suppressed serum IL-5 and blood eosinophils at 10:00 (Fig. 4a, b). To minimize the effects of altered light/dark cycle or stress induced by fasting, we restricted two groups of mice to feeding at night only or day only, allowed both groups to acclimatize for 9 days, and analysed them at 8:00 (Extended Data Fig. 6a). Unlike lung ILC2 cells, lamina propria ILC2 cells express IL-13 constitutively, and this was increased in the morning if mice had just been in a fed as opposed to fasted cycle (Fig. 4c and Extended Data Fig. 6b); the numbers of ILC2 cells remained constant (Extended Data Fig. 6c). IL-13 reporter expression by intestinal ILC2 at 8:00 was diminished after a 16-h overnight fast (Extended Data Fig. 6d) and restored by administering an evening food (but not water) gavage at 22:00 (Fig. 4d).

The response of small intestine ILC2 cells to caloric input raised the possibility that these cells could respond to hormonal cues induced by feeding. Indeed, purified intestinal ILC2 cells, most of which were R5$^+$ (Extended Data Fig. 7a), released detectable IL-5 when incubated with IL-7 alone, but increased IL-5 production with addition of vasoactive intestinal peptide (VIP) but not ghrelin or enterostatin (Fig. 4e and Extended Data Fig. 7b). The effect on lung ILC2 cells was similar (Extended Data Fig. 7c). VIP is a member of the secretin family of neuropeptides, which are expressed throughout the nervous system. They are highly expressed in intestinal neurons, coordinating pancreatic secretion with smooth muscle relaxation in response to feeding[17], and in neurons of the suprachiasmatic nucleus, relaying environmental cues necessary to synchronize central circadian oscillators[18]. VIP receptor type 2 (VPAC2)-deficient and VIP-deficient mice show similar defects in circadian behaviour[19,20], and rhythms mediated by VPAC2 are entrained by feeding[21].

We proposed that VIP might signal through VPAC2 on ILC2 cells. VIP and its receptors are also expressed by immune cells, and signals through VPAC2 have been implicated in T_H2 cell expansion, survival and cytokine production[22]. Mice deficient in VPAC2 have delayed infiltrating eosinophils with allergic challenge[23]. We detected both *VPAC1* (also called *Vipr1*) and *VPAC2* (*Vipr2*) messenger RNA in intestinal and lung ILC2 cells, whereas *VPAC2* expression was undetectable in eosinophils and low in macrophages and CD4$^+$ T cells (Fig. 4f). Comparable levels of IL-5 were induced in culture with VIP or with a VPAC2-specific agonist (Fig. 4e and Extended Data Fig. 7c)[24]. VPAC2 is a G-protein-coupled receptor that can associate with $G\alpha_s$ to activate adenylate cyclase[25]. Consistent with this, we also induced comparable IL-5 levels bypassing the receptor with dibutyryl-cAMP (Fig. 4e).

First noted in humans over 80 years ago[26], circadian variation of blood eosinophils has been linked to neuroendocrine[15] and metabolic[16] cycling. As shown here, long-lived ILC2 cells in peripheral tissues are the predominant source of circulating IL-5, and their close association with vasculature positions these cells for eosinophil recruitment. After stimulation by epithelial and/or T_H2 cytokines, lung ILC2 cells increase IL-5 and co-express IL-13, leading to local eosinophil accumulation, a process that mimics the post-prandial response of intestinal ILC2 cells to caloric intake. Furthermore, ILC2 cells express functional VPAC2 receptors, providing a potential mechanism linking these dispersed tissue-resident cells with central circadian and metabolic rhythms. Intestinal eosinophils are normal in germ-free animals[4], and IL-13$^+$ ILC2 cells are found in human fetal gut[27], indicating that these biological pathways are independent of intestinal microbiota. Although further study is needed, our findings indicate that eosinophils are linked to basal circadian oscillations through ILC2 cell activation and raise the possibility that helminthic parasites may have co-opted these fundamental pathways of host metabolic homeostasis.

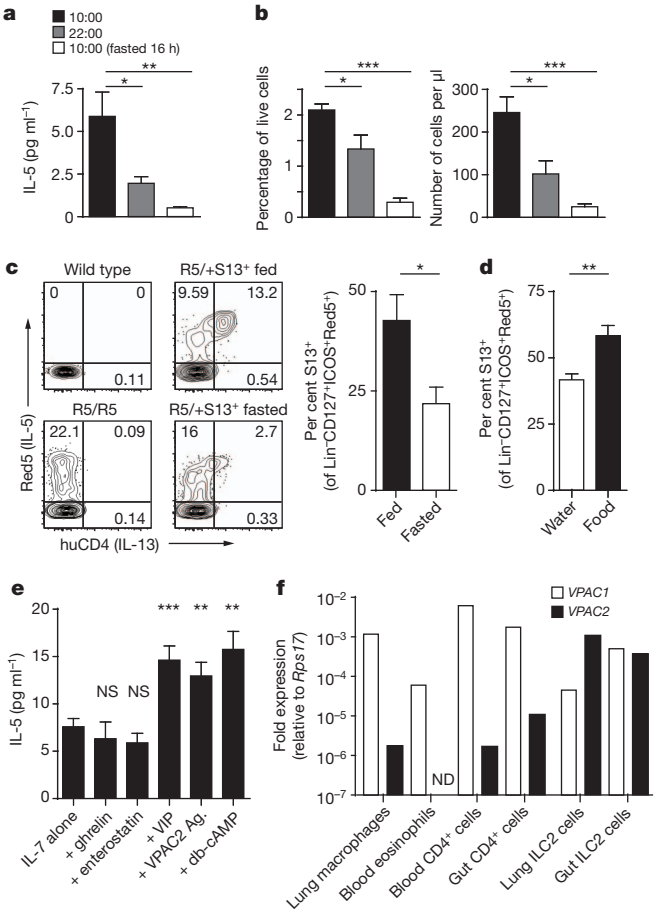

Figure 4 | ILC2 cells respond to circadian and metabolic cues. **a**, **b**, Serum IL-5 and blood eosinophils at 10:00, 22:00 or at 10:00 after fasting. **c**, **d**, Flow cytometry of small intestine ILC2 cells (Lin$^-$CD127$^+$ICOS$^+$) and percentage of R5^{hi} ILC2 cells expressing Smart13 at 8:00 in mice on night-time (black) or daytime (white) feeding (**c**) or in fasted mice given food (black) or water (white) by oral gavage (**d**). **e**, Supernatant IL-5 from intestinal Lin$^-$CD45$^+$KLRG1$^+$ ILC2 cells cultured in IL-7 alone or with indicated reagents. **f**, Expression of *VPAC1* and *VPAC2* in sorted cells, relative to *Rps17*. Data pooled from independent experiments for 19 (AM), 6 (PM), or 5 (fasted) mice per group (**a**); 7 (AM), 4 (PM), or 8 (fasted) mice per group (**b**); 8 mice per group (**c**); 6 mice per group (**d**); or pooled averages of duplicate cultures from 6 (IL-7 alone, plus VIP, plus VPAC2 agonist) or 3 (all others) cell sorts from independent mice (**e**), or representative of two experiments of independent cell sorts (**f**). Represented as mean ± s.e.m. Lin, lineage markers (B220, CD11b, CD11c, Ly6G, FcεRI and NK1.1); Rps17, 40S ribosomal protein S17; NS, not significant; $*P < 0.05$; $**P < 0.01$; $***P < 0.001$, by Student's *t*-test. db-cAMP, dibutyryl-cAMP.

METHODS SUMMARY

IL-5 reporter mice were generated as described[28], all mice on a C57BL/6 background. Tissues were mechanically dissociated, and lungs, heart, kidney, uterus, brain, intestine, skin and muscle were digested in Liberase (Roche) with or without DNase I (Roche). Some tissues were separated by 90/40 Percoll gradient (GE Healthcare). Cells were stained and analysed on an LSR II (BD) or sorted on a MoFlo XDP (Beckman Coulter). ELISA (R&D Systems) was used to detect IL-5 and CCL11, or IL-5 was detected using Enhanced Sensitivity Cytometric Bead Array (BD). BrdU was detected using a BrdU flow kit (BD Biosciences). Multiphoton imaging was performed as described[29]. Infection with 500 *N. brasiliensis* L3 larvae was as described[11]. Blood for IL-5 and eosinophils was collected as a terminal procedure. For gavage, fasted mice received water or 1:1 high-fat chow (Research Diets)[7] plus 20% dextrose at 22:00. *VPAC1* and *VPAC2* transcripts were quantified by RT–PCR[30]. All data were analysed using Prism (GraphPad Software). Paired two-tailed Student's *t*-tests were used for BrdU experiments and for *in vitro* IL-5; Kruskal–Wallis was used to compare multiple groups (Extended Data Fig. 3c); otherwise comparisons were made with unpaired two-tailed Student's *t*-tests applying Welch's correction as indicated.

Online Content Any additional Methods, Extended Data display items and Source Data are available in the online version of the paper; references unique to these sections appear only in the online paper.

Received 28 November 2012; accepted 2 August 2013.
Published online 15 September 2013.

1. Rothenberg, M. E. & Hogan, S. P. The eosinophil. *Annu. Rev. Immunol.* **24,** 147–174 (2006).
2. Takatsu, K. & Nakajima, H. IL-5 and eosinophilia. *Curr. Opin. Immunol.* **20,** 288–294 (2008).
3. Pope, S. *et al.* IL-13 induces eosinophil recruitment into the lung by an IL-5- and eotaxin-dependent mechanism. *J. Allergy Clin. Immunol.* **108,** 594–601 (2001).
4. Mishra, A., Hogan, S., Lee, J., Foster, P. & Rothenberg, M. Fundamental signals that regulate eosinophil homing to the gastrointestinal tract. *J. Clin. Invest.* **103,** 1719–1727 (1999).
5. Kopf, M. *et al.* IL-5-deficient mice have a developmental defect in $CD5^+$ B-1 cells and lack eosinophilia but have normal antibody and cytotoxic T cell responses. *Immunity* **4,** 15–24 (1996).
6. Yoshida, T. *et al.* Defective B-1 cell development and impaired immunity against *Angiostrongylus cantonensis* in IL-5Rα-deficient mice. *Immunity* **4,** 483–494 (1996).
7. Molofsky, A. B. *et al.* Innate lymphoid type 2 cells sustain visceral adipose tissue eosinophils and alternatively activated macrophages. *J. Exp. Med.* **210,** 535–549 (2013).
8. Ikutani, M. *et al.* Identification of innate IL-5-producing cells and their role in lung eosinophil regulation and antitumor immunity. *J. Immunol.* **188,** 703–713 (2012).
9. Spits, H. & Cupedo, T. Innate lymphoid cells: emerging insights in development, lineage relationships, and function. *Annu. Rev. Immunol.* **30,** 647–675 (2012).
10. Price, A. *et al.* Systemically dispersed innate IL-13-expressing cells in type 2 immunity. *Proc. Natl Acad. Sci. USA* **107,** 11489–11494 (2010).
11. Liang, H. E. *et al.* Divergent expression patterns of IL-4 and IL-13 define unique functions in allergic immunity. *Nature Immunol.* **13,** 58–66 (2012).
12. Neill, D. R. *et al.* Nuocytes represent a new innate effector leukocyte that mediates type-2 immunity. *Nature* **464,** 1367–1370 (2010).
13. Moro, K. *et al.* Innate production of TH2 cytokines by adipose tissue-associated $c\text{-}Kit^+Sca\text{-}1^+$ lymphoid cells. *Nature* **463,** 540–544 (2010).
14. Carlens, J. *et al.* Common γ-chain-dependent signals confer selective survival of eosinophils in the murine small intestine. *J. Immunol.* **183,** 5600–5607 (2009).
15. Halberg, F., Visscher, M. & Bittner, J. Eosinophil rhythm in mice: range of occurrence; effects of illumination, feeding, and adrenalectomy. *Am. J. Physiol.* **174,** 109–122 (1953).
16. Pauly, J. *et al.* Meal timing dominates the lighting regimen as a synchronizer of the eosinophil rhythm in mice. *Acta Anat.* **93,** 60–68 (1975).
17. Lelievre, V. *et al.* Gastrointestinal dysfunction in mice with a targeted mutation in the gene encoding vasoactive intestinal polypeptide: a model for the study of intestinal ileus and Hirschsprung's disease. *Peptides* **28,** 1688–1699 (2007).
18. Maywood, E. S. *et al.* Analysis of core circadian feedback loop in suprachiasmatic nucleus of mCry1-luc transgenic reporter mouse. *Proc. Natl Acad. Sci. USA* **110,** 9547–9552 (2013).
19. Harmar, A. J. *et al.* The $VPAC_2$ receptor is essential for circadian function in the mouse suprachiasmatic nuclei. *Cell* **109,** 497–508 (2002).
20. Colwell, C. S. *et al.* Disrupted circadian rhythms in VIP- and PHI-deficient mice. *Am. J. Physiol. Regul. Integr. Comp. Physiol.* **285,** R939–R949 (2003).
21. Sheward, W. J. *et al.* Entrainment to feeding but not to light: circadian phenotype of VPAC2 receptor-null mice. *J. Neurosci.* **27,** 4351–4358 (2007).
22. Voice, J. *et al.* c-Maf and JunB mediation of Th2 differentiation induced by the type 2 G protein-coupled receptor (VPAC2) for vasoactive intestinal peptide. *J. Immunol.* **172,** 7289–7296 (2004).
23. Samarasinghe, A. E., Hoselton, S. A. & Schuh, J. M. The absence of the VPAC2 receptor does not protect mice from *Aspergillus* induced allergic asthma. *Peptides* **31,** 1068–1075 (2010).
24. Tsutsumi, M. *et al.* A potent and highly selective VPAC2 agonist enhances glucose-induced insulin release and glucose disposal: a potential therapy for type 2 diabetes. *Diabetes* **51,** 1453–1460 (2002).
25. Dickson, L. & Finlayson, K. VPAC and PAC receptors: From ligands to function. *Pharmacol. Ther.* **121,** 294–316 (2009).
26. Domarus, A. v. Die bedeutung der kammerzahlung der eosinophilen fur die klinik. *Dtsch. Arch. Klin. Med.* **171,** 333–358 (1931).
27. Mjösberg, J. M. *et al.* Human IL-25- and IL-33-responsive type 2 innate lymphoid cells are defined by expression of CRTH2 and CD161. *Nature Immunol.* **12,** 1055–1062 (2011).
28. Sullivan, B. M. *et al.* Genetic analysis of basophil function *in vivo*. *Nature Immunol.* **12,** 527–535 (2011).
29. Thornton, E. E. *et al.* Spatiotemporally separated antigen uptake by alveolar dendritic cells and airway presentation to T cells in the lung. *J. Exp. Med.* **209,** 1183–1199 (2012).
30. Vomhof-DeKrey, E. E. *et al.* Radical reversal of vasoactive intestinal peptide (VIP) receptors during early lymphopoiesis. *Peptides* **32,** 2058–2066 (2011).

Acknowledgements We thank the NIH Tetramer Core Facility for reagents, B. Sullivan, N. Flores, M. Consengco and Z. Wang for technical expertise, and M. Anderson, C. Lowell and M. McCune for comments on the manuscript. Supported by NIH (AI026918, AI030663, AI078869, HL107202), the Diabetes Endocrinology Research Center grant (DK063720), the Howard Hughes Medical Institute and the Sandler Asthma Basic Research Center at the University of California San Francisco. J.C.N. is supported by NIH training grants (AI007641 and AI007334).

Author Contributions J.C.N. performed experiments, interpreted data and wrote the manuscript; L.E.C. provided experimental and imaging assistance; S.J.V.D., A.M., A.B.M. and J.v.M. provided experimental assistance; E.E.T. performed imaging assays; M.F.K. provided reagents and expertise; H.-E.L. generated mouse cytokine reporter strains; A.C. discussed experiments and provided oversight for metabolic studies; R.M.L. directed the studies and wrote the paper with J.C.N.

Author Information Reprints and permissions information is available at www.nature.com/reprints. The authors declare no competing financial interests. Readers are welcome to comment on the online version of the paper. Correspondence and requests for materials should be addressed to R.M.L. (locksley@medicine.ucsf.edu).

METHODS

IL-5 reporter mice. R5 IL-5 reporter mice were generated by homologous gene targeting in C57BL/6 embryonic stem cells. The previously published plasmid pKO915-DT (Lexicon) containing the Basoph8 reporter[17] was modified to express tdTomato in place of YFP, such that the cassette now contained (in order from 5′ to 3′) genomic sequence of the rabbit β-globin gene partial exon 2-3, the gene encoding tdTomato (Clontech), encephalomyocarditis virus IRES, humanized Cre recombinase, bovine growth hormone poly(A), and a *loxP*-flanked neomycin resistance cassette. Homologous arms straddling the *Il5* translation initiation site (3.8 kilobases (kb) towards 5′, containing the promoter and 5′ UTR and 3.0 kb towards 3′, containing the start ATG halfway through exon 3) were amplified from C57BL/6 genomic DNA using Phusion polymerase (Finnzymes) and cloned into the cassette by standard methods. The construct was linearized with NotI and transfected by electroporation into C57BL/6 embryonic stem cells. Cells were grown on irradiated feeders with the aminoglycoside G418 in the media, and neomycin-resistant clones were screened for 5′ and 3′ homologous recombination by PCR. Eleven positive clones were subsequently tested (and all eleven confirmed) by 5′ and 3′ Southern blot. Two clones were selected for injection into albino C57BL/6 blastocysts to generate chimaeras, and the male pups with highest ratios of black-to-white coat colour from a single clone were selected to breed with homozygous CMV-Cre transgenic C57BL/6 females (B6.C-Tg(CMV-Cre)1Cgn/J; 006054, obtained from The Jackson Laboratory) to excise the neomycin resistance cassette. The CMV-Cre transgene is X-linked and the males from this cross were bred to wild-type C57BL/6 females to remove the CMV-Cre allele. Male and female R5/+ offspring were intercrossed to yield R5/R5 homozygotes.

Mice. β-actin-cyan fluorescent protein mice (B6.129(ICR)-Tg(CAG-ECFP)CK6Nagy/J; 004218), *Rag1*$^{-/-}$ mice (B6.129S7-*Rag1*^{tm1Mom}/J; 002216), *Il7ra*$^{-/-}$ mice (B6.129S7-*Il7r*^{tm1Imx}/J; 002295), and ROSA-YFP mice (B6.129X1-*Gt(ROSA)26Sor*$^{tm1(EYFP)Cos}$/J; 006148) were from The Jackson Laboratory. ROSA-DTα and Smart13 mice have been described[11]. *Rag1*$^{-/-}$ mice were maintained on SCIDS MD's 'Breeders Formula' antibiotic tablets (Bio-Serv). Mice were fed ad libitum except when feeding was restricted to 12 h daily (7:00 to 19:00 or vice versa) or during 16-h fasting. For gavage experiments, mice previously fed standard chow ad libitum were fasted at 16:00 before receiving water or a 1:1 mixture of high-fat chow (Research Diets) and 20% dextrose by oral gavage, representing 13% of ad libitum caloric intake at 22:00. Mice used in experiments were mixed gender, between 6 and 10 weeks old, on the C57BL/6 background and were maintained according to institutional guidelines in specific pathogen-free facilities at the University of California, San Francisco.

***Nippostrongylus brasiliensis* infection and cytokine administration.** Mice were infected with 500 *N. brasiliensis* third-stage larvae (L3) and were killed at the indicated time points for analysis of the mediastinal and mesenteric lymph nodes, lungs and bone marrow. Procedures for maintaining are as described previously[11]. *Rag1*$^{-/-}$ mice were given IL-2, IL-33 and IL-13 as follows: IL-2 complexes were generated by incubating 0.5 μg mouse IL-2 (R&D Systems) with 5 μg anti-IL2 (JES6-A12, R&D Systems), and then administered intraperitoneally in 200 ml PBS on day 0; IL-33 was given in two daily doses of 500 ng in 30 μl PBS intranasally on days 0 and 1; some animals additionally received 1 μg of IL-13 intranasally with the daily doses of IL-33 on days 0 and 1. On day 2, the lungs were collected. The left lobe was treated as above and cells were isolated for flow cytometry. The right lung was homogenized in 1 ml of PBS using GentleMACS C tubes (Miltenyi Biotec), pelleted, and the supernatant was filtered through a 0.8 μm strainer and used for CCL11 ELISA (R&D Systems).

***In vitro* CD4$^+$ T-cell polarization.** CD4$^+$ T cells were isolated from the lymph nodes of R5/R5, R5/+ and wild-type C57BL/6 mice using negative selection MACS beads (Miltenyi Biotec) and cultured in plates pre-coated with anti-CD3ε and anti-CD28 (BD Pharmingen) under standard T_H2 polarization conditions for four days, as described[11]. On day 4 the cells were washed and re-plated with 50 U ml^{-1} recombinant human IL-2 (R&D Systems) and then split at day 6 and day 8. On day 9 or 10, the cells were plated at 2×10^6 ml^{-1} in plates pre-coated with anti-CD3ε. One well was used for intracellular cytokine staining: 3 μM monensin was added at 18 h, and at 24 h the cells were stained with phycoerythrin-cyanine 7 (PE-Cy7) anti-CD3 (17A2, eBioscience) and peridinin chlorophyll protein-cyanine 5.5 (PerCP-Cy5.5) anti-CD4 (RM4-5, eBiosciences) and with Violet LIVE/DEAD (Invitrogen) before fixation in 2% paraformaldehyde (PFA, Electron Microscopy Sciences) in PBS, permeabilization with 0.5% saponin/3% fetal calf serum (FCS) in PBS, and staining with allophycocyanin (APC) anti-IL-5 (TRFK5, BD Pharmingen), fluorescein (FITC) anti-IFN-γ (XMG1.2, BD Pharmingen), eFluor 660 anti-IL-13 (50-7133-80, eBioscience), or PE anti-IL-4 (11B11, BD Pharmingen). For the remaining wells, re-stimulation on anti-CD3ε was continued for 4 days and each day supernatant was collected and stored at −20 °C, and one well was collected for flow cytometry.

Cell preparation from tissues. We performed transcardiac perfusion with 20 ml of PBS before harvesting organs. Single-cell suspensions were prepared as follows: spleen, lymph nodes and thymus were mechanically dissociated through 70 μm filters and bone marrow was processed by crushing a single femur with a mortar and pestle before 70-μm filtration. Whole lungs, heart, kidney and uterus were minced, digested by gentle shaking in 5 ml HBSS with 0.1 Wünsch units (WU) ml^{-1} Liberase (Roche) and 25 μg ml^{-1} DNase I (Roche) for 30 min at 37 °C, and then mechanically dissociated using GentleMACS C tubes (Miltenyi Biotec) followed by a 70 μm filter. Brain and skeletal muscle were similarly digested in Liberase/DNase, but were re-suspended in 40% Percoll (GE Healthcare), underlaid with 90% Percoll and centrifuged at 2,200 r.p.m. for 20 min at 20 °C to isolate the haematopoietic cells from the interphase. Liver was minced, passed through a 70-μm filter and separated using a 90/40 Percoll gradient without enzymatic digestion. Skin and small intestinal lamina propria were prepared as described[28]. Peyer's patches were treated like lymph nodes (see above). Cells from all tissues were washed with PBS containing 3% (v/v) FCS and 1 mg l^{-1} sodium azide.

Flow cytometry. The single-cell suspensions prepared above were pelleted and incubated with anti-CD16/CD32 monoclonal antibodies (UCSF Antibody Core Facility) for 10 min at 4 °C. The cells were stained with antibodies to surface markers for 25 min at 4 °C and, if necessary, were washed and incubated with secondary antibodies for an additional 25 min at 4 °C. After a final wash, cells were re-suspended in 1 μg ml^{-1} 4',6-diamidino-2-phenylindole (DAPI, Roche) for dead cell exclusion. Monoclonal antibodies from Biolegend included: Pacific blue anti-Ly-6G/Ly-6C (Gr-1), Pacific blue anti-CD3 (17A2), Pacific blue anti-CD8α (53-6.7), Pacific blue anti-CD11b (M1/70), Pacific blue anti-CD11c (N418), Pacific blue anti-NK1.1 (PK136), Alexa Fluor 488 anti-CD3 (17A2); FITC anti-FcεRIα (MAR-1); PerCP-Cy5.5 anti-CD11c (N418), and anti-Gr-1 (RB6-8C5); Brilliant violet 605 anti-CD4 (RM4-5) and anti-CD11b (M1/70); Brilliant violet 711 anti-CD4 (RM4-5); Alexa Fluor 647 anti-FcεRIα (MAR-1); APC anti-KLRG1 (2F1), anti-ICOS (C398.4A), and anti-CD45R/B220 (RA3-6B2); APC-Cy7 anti-CD25 (PC-61) and anti-CD45 (30-F11); and biotinylated anti-ICOS (C398.44). Monoclonal antibodies from eBioscience included: Alexa Fluor 647 anti-CD19 (eBio1D3); APC anti-NK1.1 (PK136); PE-Cy7 anti-CD5 (53-7.3); APC-eFluor 780 anti-CD11b (M1/70) and anti-CD90.2 (53-2.1); PerCP-eFluor 710 anti-KLRG1 (2F1); PerCP-Cy5.5 anti-CD127 (A7R34); APC anti-human CD4 (RPA-T4) was used to detect human CD4 expressed in Smart13 mice. Monoclonal antibodies from BD Biosciences included: FITC anti-TCRβ (H57-597); PerCP-Cy5.5 anti-CD11b (M1/70), anti-CD19 (1D3), and anti-CD8α (53-6.7); Alexa Fluor 647 anti-SiglecF (E50-2440); APC anti-CD11c (HL3); APC-Cy7 anti-Gr-1 (RB6-8C5); PE-Cy7 anti-CD11c (HL3) and anti-NK1.1 (PK136); Horizon V500 anti-CD4 (RM4-5) and anti-CD45 (30-F11); and biotinylated anti-KLRG1 (2F1). Monoclonal antibodies from Invitrogen included APC anti-Gr-1 (RB6-8C5) and APC Alexa Fluor 750 anti-CD45R/B220 (RA3-6B2). FITC and biotinylated anti-T1/ST2 (DJ8) were from MD Bioproducts. An Alexa Fluor 488-conjugated anti-SiglecF antibody was generated using purified anti-SiglecF (E50-2440, BD Pharmingen) with an Alexa Fluor 488 monoclonal antibody labelling kit (Invitrogen). Secondary antibodies included streptavidin V500 (BD Horizon), streptavidin BV 605 and BV 650 (Biolegend). Cell counts were performed using CountBright beads (Invitrogen). Samples were analysed on an LSR II (BD Biosciences) with four lasers (403 nm, 488 nm, 535 nm, and 633 nm) and data were analysed with FlowJo software (Treestar).

Lung imaging. Lung slices were prepared using a modification of established methods[29]. After euthanasia, lungs were inflated with 1 ml of 2% low-melt agarose (Type VII, Sigma-Aldrich), excised and placed in 5 ml cold PBS, and 600 μm sections were cut on a vibratome (Model G, Oxford Laboratories). Lung sections were maintained in PBS at room temperature until mounting. All sections were mounted with PBS and imaged on a multiphoton microscope with data collected in three channels (CFP, GFP, RFP). Images were analysed with Imaris software (Bitplane). Software spot detection algorithms were used to identify cells.

BrdU. Naive mice received 300 μg BrdU (Sigma-Aldrich) in 300 μl PBS as an intraperitoneal injection on the day that their standard drinking water was exchanged for water containing 800 μg ml^{-1} BrdU and 220 μg ml^{-1} sodium saccharin (Sigma-Aldrich). The water bottles were covered in aluminium foil and water was changed every 3 days. On the indicated days, lungs and thymus were collected. Single-cell suspensions were prepared as above and cells were stained with antibodies for surface markers followed by violet fixable LIVE/DEAD (Invitrogen). Cells were then fixed in 4% PFA in PBS at room temperature for 15 min, followed by staining for BrdU incorporation using the APC BrdU Flow Kit (BD Biosciences).

ILC2 cell culture. ILC2 cells from lungs and small intestines of mice were sorted on a MoFlo XDP gating on cells negative for lineage markers (CD3, CD4, CD5, CD8, CD19, CD11b, CD11c, Gr-1, NK1.1), followed by CD90.2$^+$R5$^+$ selection (lung) or Lin$^-$KLRG1$^+$R5$^+$ selection (intestine). In some experiments, wild-type organs were prepared and gated on cells negative for lineage markers (as above), followed by CD90.2$^+$CD25$^+$ selection (lung) or CD45$^+$KLRG1$^+$ selection (intestine). For Elispot, cells were cultured at 3,000 per well in 10 ng ml^{-1} IL-7 for 48 h. For supernatant IL-5, cells were cultured at 5,000 per well for 18 h, or at 10,000 per well

for 6 h, in 10 ng ml^{-1} IL-7 plus 1 μM VIP, VPAC2-specific agonist (BAY 55-9837), ghrelin, or enterostatin or 100 μM dibutyryl cAMP.

IL-5 detection. Supernatant from T-cell cultures was assayed for IL-5 by ELISA, performed in duplicate serial twofold dilutions using IL-5 Duoset (R&D Systems). For Elispot, ILC2 cells were plated at 3,000 per well in a 96-well Multiscreen filter plate (Millipore) pre-coated with anti-IL-5 capture antibody (eBiosience). The cells were cultured in complete RPMI-10% FCS and after 48 h the wells were washed and treated according to the manufacturer's ELISPOT protocol (eBioscience). IL-5 from serum and ILC2 cell culture supernatant was measured using an Enhanced Sensitivity Flex Set with Enhanced Sensitivity Cytometric Bead Array kit (BD). Bead fluorescence was captured on an LSRII (BD) and analysed using Flow Cytometric Analysis Program (FCAP) Array software (BD).

Quantitative RT–PCR. ILC2 cells (see above), lung macrophages (CD11b^{+}CD11c^{+}), blood eosinophils (SiglecF^{+}CD11b^{+}SSC^{hi}), and blood and intestinal CD4^{+} cells were sorted on a MoFlo XDP and RNA was isolated using the Micro RNeasy kit (Qiagen). The RNA was reverse transcribed with SuperScript III (Invitrogen), and the resulting cDNA was used as template for quantitative PCR with the Power SYBR Green kit on a StepOnePlus cycler (Applied Biosystems). Intron-spanning *VPAC1* and *VPAC2* primers were as described[30]. Transcripts were normalized to 40S ribosomal protein S17 (*Rps17*) (sense: 5′-CGCCATTATCCCCAGCAAG-3′; antisense: 5′-TGTCGGGATCCACCTCAATG-3′).

Experimental design and statistics. All experiments comparing treatment groups were made using randomly assigned littermates without investigator blinding. Comparisons among mice of different litters were made using age- and gender-matched cohorts. Cohort sizes were chosen after estimating effect size and consulting power tables, and data were analysed for statistical significance after at least two repeated experiments. Results from independent experiments performed similarly were pooled. All data points reflect biological replicates; technical replicates were averaged to yield a single value for analysis. No data were excluded. All data were analysed using Prism (GraphPad Software): to compare means in BrdU experiments and ILC2 cell culture supernatants we used paired two-tailed Student's *t*-tests and significance was defined as $P < 0.05$. Comparison across multiple groups in Extended Data Fig. 3c was performed using Kruskal–Wallis. Otherwise, all data were analysed by comparison of means using unpaired two-tailed Student's *t*-tests. If the groups to be compared had significantly different variances ($P < 0.05$ by F test) then Welch's post-test was performed. Figures display means ± s.e.m. unless otherwise noted.

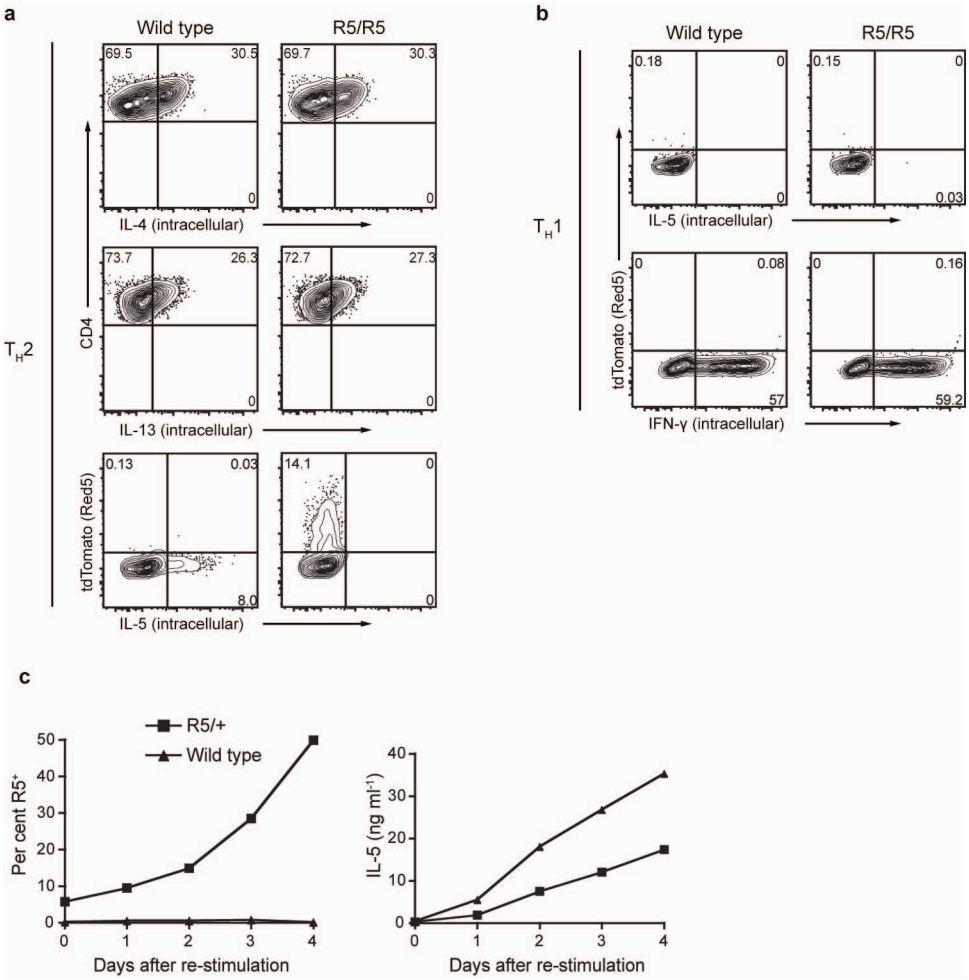

Extended Data Figure 1 | Performance of R5 reporter in T-cell cultures. **a**, **b**, Flow cytometry with intracellular staining for IL-4, IL-13, IL-5 and IFN-γ of $CD4^+$ T cells from wild-type and R5/R5 mice cultured under T_H2 (**a**) or T_H1 (**b**) conditions and then re-stimulated for 24 h. Numbers represent per cent of $CD3^+CD4^+$ cells. **c**, Percentage of cultured $CD3^+CD4^+$ cells in the $R5^+$ gate and ELISA for IL-5 from the supernatants in R5/+ and wild-type T_H2 cultures re-stimulated on plate-bound anti-CD3ε for 4 days. Data are representative of two independent experiments (**a**, **b**), and ELISA data (**c**) obtained by averaging four replicates per time point.

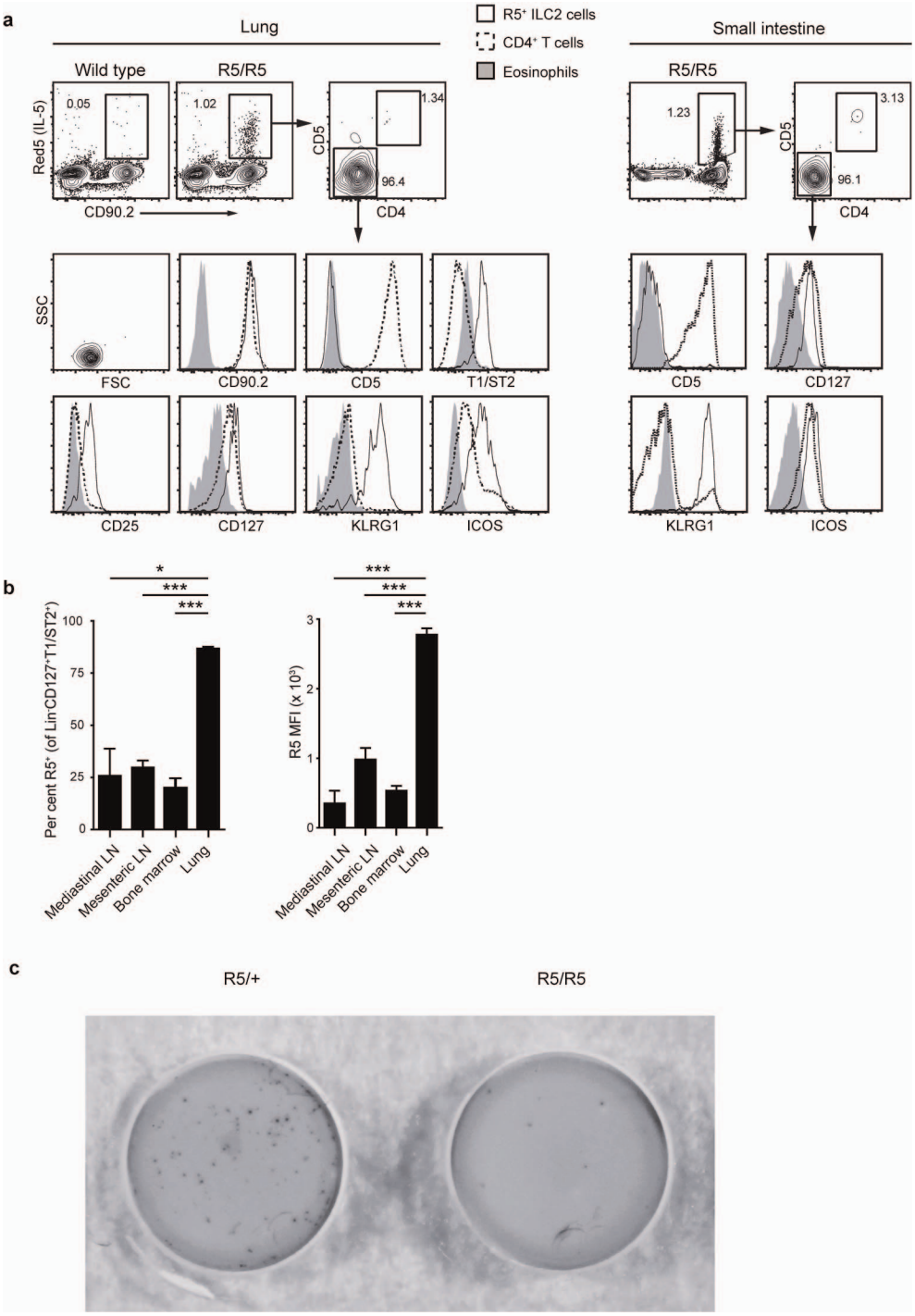

Extended Data Figure 2 | Surface markers and R5 expression in resting ILC2 cells. **a**, Gating of cells from lung and small intestine. Numbers in first two panels (lung) and first panel (intestine) are percentage of live ($DAPI^-$) cells, and remaining panel previously gated on $R5^+CD90.2^+$ cells (lung) or $R5^+CD45^+$ cells (intestine). Histograms show $R5^+CD4^-CD5^-$ cells, total $CD4^+CD5^+$ cells, and eosinophils ($SiglecF^+CD11b^+SSC^{hi}$). **b**, Percentage $R5^+$ of $Lin^-CD127^+T1/ST2^+$ cells and R5 fluorescence in indicated tissues. **c**, IL-5 ELISPOT of $R5^+$ cells sorted from the lungs of R5/+ or R5/R5 mice and cultured (3,000 cells per well) for 48 h. Data are representative of two independent experiments with three mice per group (**a**, **b**), or representative of two independent experiments using sorted cells pooled from four mice (**c**). Represented as mean ± s.e.m. Lin, lineage markers (B220, CD5, CD11b, CD11c, Ly6G, FcεRI and NK1.1); MFI, mean fluorescence intensity; $*P < 0.05$; $***P < 0.001$, by Student's *t*-test.

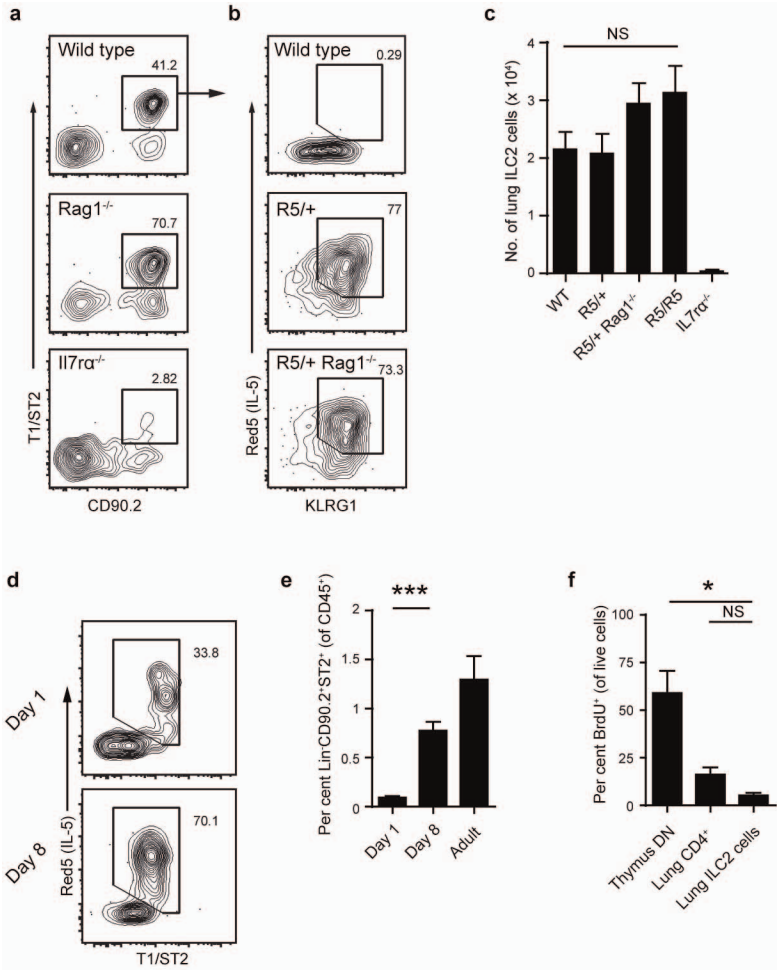

Extended Data Figure 3 | R5$^+$ ILC2 cells require IL-7 and appear and persist after birth. **a**, Flow cytometry of lung cells from mouse strains as indicated. Numbers are percentage of Lin$^-$ cells. **b**, Flow cytometry of lung cells previously gated as in **a** (Lin$^-$CD90.2$^+$T1/ST2$^+$). Numbers are percentage of Lin$^-$CD90.2$^+$T1/ST2$^+$ cells. **c**, Total lung ILC2 cells (Lin$^-$CD90.2$^+$T1/ST2$^+$) in mouse strains as indicated. **d**, Flow cytometry of R5/+ lung; previously gated on Lin$^-$CD90.2$^+$ cells. **e**, Lung Lin$^-$CD90.2$^+$T1/ST2$^+$ cells as a percentage of CD45$^+$ cells at neonatal day 1, day 8, or week 8 of life. **f**, Per cent BrdU$^+$ of thymus CD4$^-$CD8$^-$ (DN) cells, lung CD4$^+$ T cells, and lung R5$^+$ ILC2 cells after 14 days BrdU. Data are representative of two independent experiments (**a**, **b** and **d**); pooled from three independent experiments for 4 (wild type and IL7r$\alpha^{-/-}$) or 7 (all others) mice per group (**c**); pooled from three independent experiments for 5 (day 1), 6 (day 8), or 4 (adult) mice per group (**e**); or pooled from two independent experiments for 3 mice per group (**f**). Represented as mean ± s.e.m. Lin, lineage markers (B220, CD5, CD11b, CD11c, Ly6G, FcεRI and NK1.1); NS, not significant by Kruskal–Wallis (**c**) or by Student's *t*-test (**f**); *$P < 0.05$; ***$P < 0.001$, by Student's *t*-test.

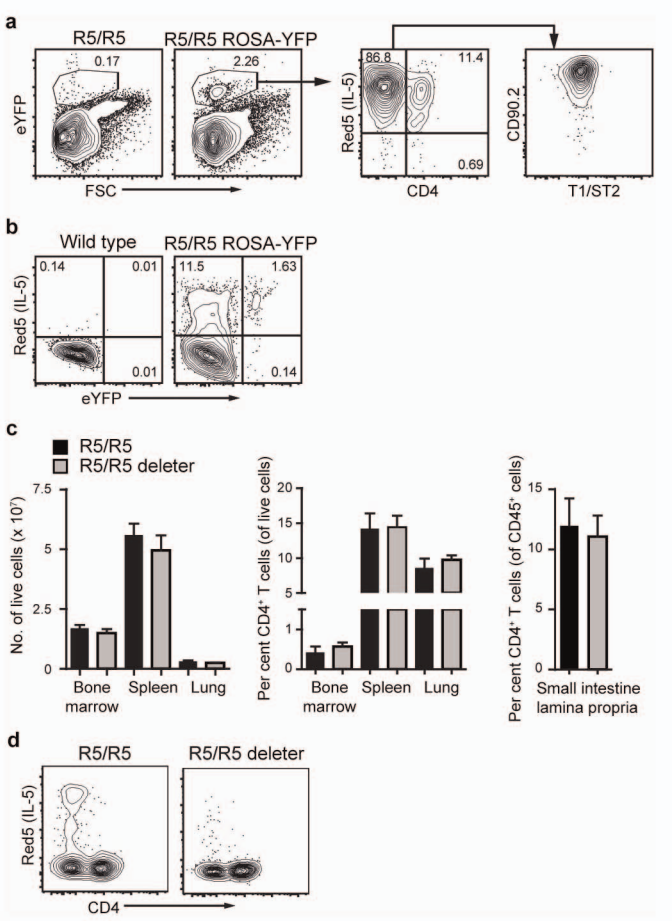

Extended Data Figure 4 | Cre-mediated tracking or deletion of R5$^+$ cells. **a**, **b**, Flow cytometry of R5/R5 and R5/R5 ROSA–YFP lungs 12 days after infection with *N. brasiliensis*, previously gated on live (DAPI$^-$) cells. **a**, Numbers are per cent YFP$^+$ of live (DAPI$^-$) cells (left two panels), and per cent R5$^+$CD4$^+$ and R5$^+$CD4$^-$ of YFP$^+$ cells (second from right). Far right panel, CD90.2 and T1/ST2 staining of R5$^+$CD4$^-$ cells. **b**, Numbers are per cent of CD4$^+$ cells. **c**, Baseline total cells and per cent CD4$^+$ T cells in bone marrow (single femur), spleen and lung, and CD4$^+$ cells as a per cent of CD45$^+$ cells in small intestine lamina propria of R5/R5 or R5/R5 deleter mice. **d**, Representative flow cytometry of small intestine lamina propria cells (previously gated as CD45$^+$CD8$^-$NK1.1$^-$). Data are representative of 2 mice in each group from one experiment (**a**, **b**); or pooled from three independent experiments for 6 (small intestine, and R5/R5 bone marrow and spleen) or 9 (all others) mice per group (**c**); or representative of two mice in each group from one experiment (**d**). Represented as means ± s.e.m. BM, bone marrow; ***$P < 0.001$ by Student's *t*-test.

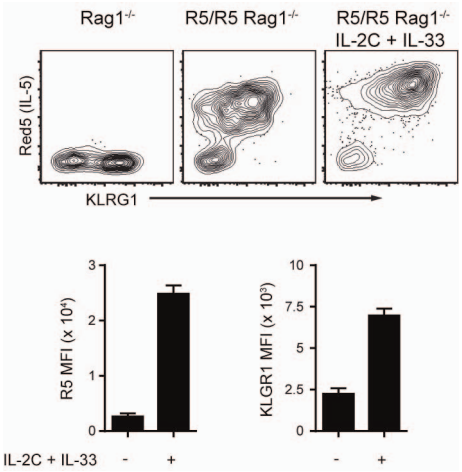

Extended Data Figure 5 | Activation by IL-2 and IL-33. Flow cytometry and quantification of R5 and KLRG1 fluorescence in ILC2 cells from untreated *Rag1*$^{-/-}$ and R5/R5 *Rag1*$^{-/-}$ mice, and R5/R5 *Rag1*$^{-/-}$ mice treated with IL-2 and IL-33. Lung cells previously gated as Lin^{-}CD90.2^{+}. Data are pooled from two independent experiments for 3 (R5/R5 + PBS) or 8 (R5/R5 + IL-2/IL-33) mice per group. Represented as means ± s.e.m. MFI, mean fluorescence intensity.

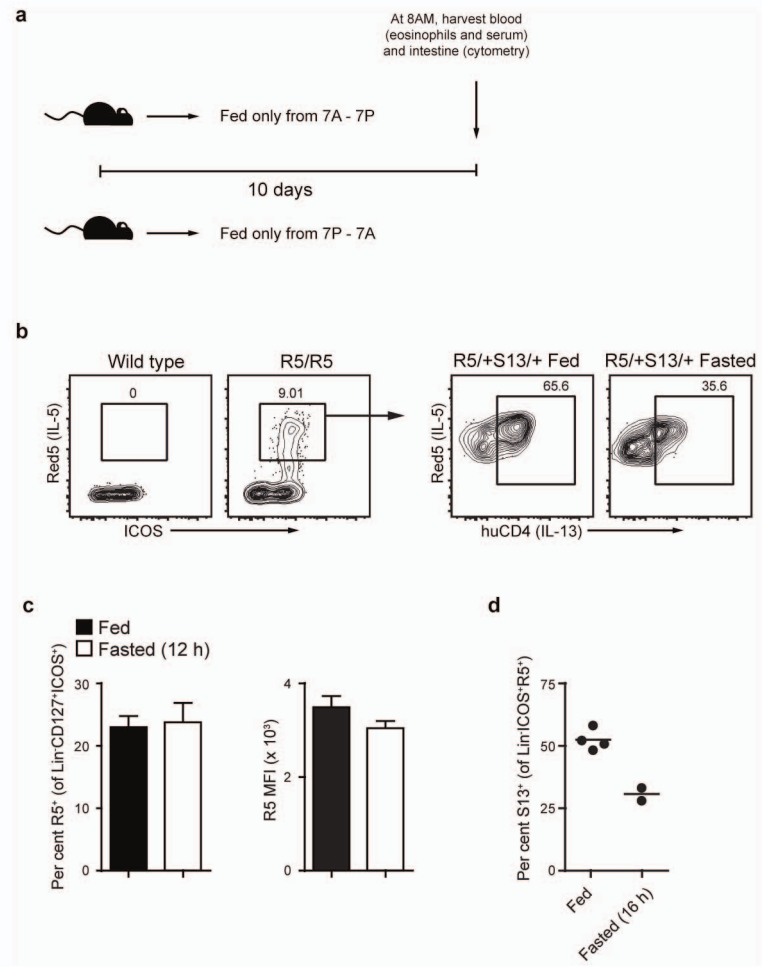

Extended Data Figure 6 | Feeding enhances Smart13 expression. **a**, Schematic for feeding during light-only or dark-only 9 days before collecting tissues. **b**, Flow cytometry of small intestine cells previously gated on $CD45^+Lin^-CD127^+$ (left panels), or $CD45^+Lin^-CD127^-ICOS^+R5^+$ (right panels) showing human CD4 and R5 fluorescence. **c**, Per cent $R5^+$ and R5 fluorescence of lamina propria ILC2 cells after 10-day food schedule in **a**. **d**, Per cent $Smart13^+$ (S13) of lamina propria after 16-h fast. Data are representative of 2 independent experiments with 4 mice per group (**b**, **c**), or one experiment with 4 (fed) or 2 (fasted) mice per group (**d**). Represented as mean ± s.e.m. Lin, lineage markers (CD4, CD5, CD8, B220, CD11b, CD11c, NK1.1, Gr1); MFI, mean fluorescence intensity.

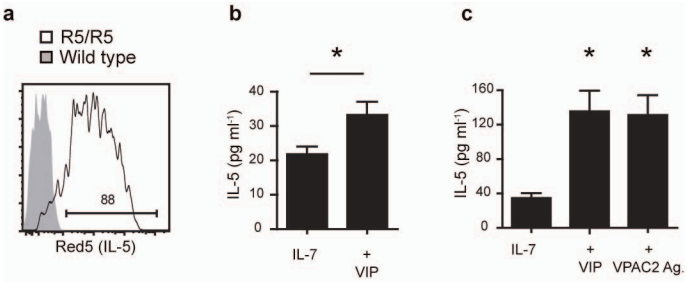

Extended Data Figure 7 | Sorted ILC2 cells respond to VIP.
a, Representative flow cytometry of ILC2 cells from small intestine of wild-type or R5/R5 mice, previously gated on $Lin^{-}CD45^{+}KLRG1^{+}$. **b**, **c**, IL-5 in culture supernatant measured by cytometric bead array. **b**, $Lin^{-}CD45^{+}KLRG1^{+}$ ILC2 cells sorted from small intestine cultured at 10,000 per well in IL-7 (10 ng ml^{-1}) alone or with VIP (1 μM) for 6 h. **c**, $Lin^{-}CD90.2^{+}CD25^{+}$ ILC2 cells sorted from lung cultured at 5,000 per well in IL-7 (10 ng ml^{-1}) alone or with VIP or VPAC2-specific agonist BAY 55-9837 (both 1 μM) for 18 h. Data are representative of three independent experiments (**a**) or pooled averages of duplicate cultures from 4 (**b**) or 3 (**c**) independent cell sorts. Represented as mean ± s.e.m. Lin, lineage markers (CD4, CD5, CD8, B220, CD11b, CD11c, NK1.1, Gr1); $*P < 0.05$ by paired Student's *t*-test.